Nanoscale Energy-Filtered Scanning Confocal Electron Microscopy Using a Double-Aberration-Corrected Transmission Electron Microscope

Peng Wang,[1] Gavin Behan,[1] Masaki Takeguchi,[2] Ayako Hashimoto,[2] Kazutaka Mitsuishi,[2] Masayuki Shimojo,[3] Angus I. Kirkland,[1] and Peter D. Nellist[1,*]

[1]*Department of Materials, University of Oxford, Parks Road, Oxford OX1 3PH, United Kingdom*
[2]*National Institute for Materials Science, 3-13 Sakura, Tsukuba, 305-0003, Japan*
[3]*Advanced Science Research Laboratory, Saitama Institute of Technology, 1690 Fusaiji, Fukaya 369-0293, Japan*

(Received 6 November 2009; published 20 May 2010)

We demonstrate that a transmission electron microscope fitted with two spherical-aberration correctors can be operated as an energy-filtered scanning confocal electron microscope. A method for establishing this mode is described and initial results showing 3D chemical mapping with nanoscale sensitivity to height and thickness changes in a carbon film are presented. Importantly, uncorrected chromatic aberration does not limit the depth resolution of this technique and moreover performs an energy-filtering role, which is explained in terms of a combined depth and energy-loss response function.

DOI: 10.1103/PhysRevLett.104.200801 PACS numbers: 07.78.+s, 41.85.−p, 68.37.−d, 79.20.Uv

Confocal scanning optical microscopy is an established technique in light optics [1]. It makes use of the small depth of focus of high numerical-aperture (NA) lenses to ''section'' a sample allowing depth discrimination and acquisition of three-dimensional (3D) information. In a conventional microscope, the scattering from regions of the sample away from the focal plane still contributes to the image as an out-of-focus blur. In the confocal configuration, however, both the incident and scattered light are passed through high NA optics that are focused at the same plane. An aperture is arranged optically conjugate to the selected plane and only scattering from this plane is focused at this aperture [Fig. 1(a)]. The out-of-focus blurring is removed and the depth resolution and discrimination are improved. An electron analogue to confocal scanning optical microscopy offers the potential for significant improvement in 3D resolution. In the first attempt at an electron analogue, the scanning confocal electron microscope (SCEM), Frigo *et al.* [2] have shown improved image contrast in very thick specimens. However, their depth of field was severely limited by the restricted NA due to inherent spherical aberration in round electromagnetic lenses [3].

Spherical-aberration correctors for both transmission electron microscopy (TEM) [4] and scanning TEM (STEM) [5] have dramatically improved the lateral resolution of 2D images [6]. Corrected optics also reduce the depth of field to a few nanometers, allowing measurement of the height of single heavy atoms in a light support matrix [7] using STEM in a high angle annular dark field imaging mode. However, recent work [8] has shown that the depth resolution in this imaging mode rapidly deteriorates for laterally extended objects because of a ''missing cone'' in the three-dimensional optical transfer function (OTF) [9]. In contrast, the incoherent confocal mode does not suffer from a missing cone in the OTF [1,10] leading to improved depth discrimination for laterally extended objects while retaining maximum depth resolution.

The simplest confocal mode detecting elastically scattered electrons is referred to as bright-field (BF) SCEM. Nellist *et al.* [11] have demonstrated BFSCEM confocal trajectories in a TEM-STEM instrument fitted with two spherical-aberration correctors [Fig. 1(a)]. Adding an energy filter to detect electrons that have been inelastically scattered with a specific energy loss in the sample leads to energy-filtered SCEM (EFSCEM). Cosgriff *et al.* [12] have shown that the overall image contrast of BFSCEM is inherently weak and difficult to interpret. This problem does not occur with the EFSCEM mode because the scattering is largely incoherent, and moreover, this optical geometry gives atomic species selectivity that in principle allows 3D elemental mapping on a nanometer scale [13].

A significant difficulty in the implementation of EFSCEM arises from the residual uncorrected chromatic

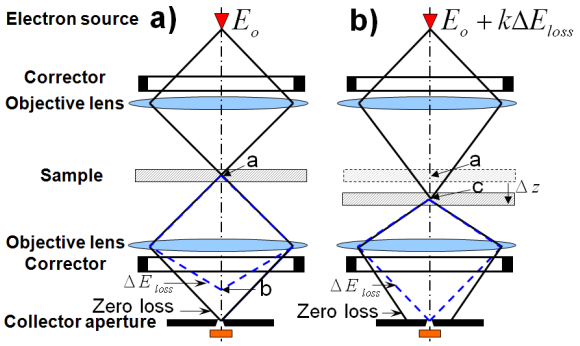

FIG. 1 (color online). Schematic diagrams of confocal trajectories (a) BFSCEM (solid lines). Because of C_c the postspecimen optics focuses beams (dashed lines) with an energy loss ΔE_{loss} at point b; (b) EFSCEM. An increment, $k\Delta E_{\mathrm{loss}}$ applied to the accelerating voltage E_0 reestablishes a new confocal point c for beams (dashed lines) with an energy loss, ΔE_{loss}.

aberration (referred to here by its mathematical coefficient C_c) in electron lenses. Direct C_c correction is technologically challenging and expensive[14]. Chromatic aberration, changes the focal length of a lens by $\Delta z = \Delta E_{\text{loss}} C_c / E_0$ for inelastic electrons with an energy loss of ΔE_{loss} relative to the elastically scattered electrons. Furthermore, typical EFTEM images are recorded with energy losses that range over a window of several eV to ensure sufficient signal [15] and for typical values of C_c = 1.5 mm, $\Delta E_{\text{window}} = 10$ eV, and $E_0 = 200$ keV, the resulting focal spread is 75 nm; much greater than the 3.5 nm depth of focus predicted in Ref. [11] for an EFSCEM experiment.

A method for the electron optical alignment for the BFSCEM mode has been described previously [11]. For EFSCEM, electrons with a desired energy loss are focussed prematurely by the postspecimen optics because of C_c [Fig. 1(a)]. In principle, the postspecimen optics could be adjusted to compensate for this effect. However, in practice, this would require a change in focal length of the postspecimen optics of several microns, resulting in an unacceptable optical misalignment. Furthermore, accurate adjustment of magnetic lenses at the level required would be hindered by a lack of reproducibility due to magnetic hysteresis. An alternative approach is to adjust the energy of the incident electrons by simply adjusting the accelerating voltage. It is accurate and reproducible, and appears to result in a smaller degree of optical misalignment.

Having established confocal trajectories at the primary beam energy, the confocal condition for inelastic electrons with an energy loss, ΔE_{loss}, can be regained by increasing the incident electron energy, E_0, by $k\Delta E_{\text{loss}}$ [Fig. 1(b)] where

$$k = C_{c2}/(C_{c1} + C_{c2}) \tag{1}$$

and where, C_{c1} and C_{c2} are the C_c coefficients of the pre and postspecimen optics, respectively. The focal length of the prespecimen optics is therefore increased, and compensates for the shorter focal length of the postspecimen optics for the energy-loss electrons (see, supplementary material [16] for a derivation of k).

To compare the z response of EFSCEM and conventional energy-filtered STEM (EFSTEM) for an extended object, we have used a thin amorphous carbon film (see, supplementary material [16] for the experimental conditions), for which independent measurement gave a sample thickness in the range 25 ± 5 nm. Figure 2 shows 1D scans in the z direction. The EFSTEM data was recorded with a 20 eV energy selecting window (ESW), centered at an energy loss of 290 eV in order to record the carbon K edge. As predicted from the missing cone in the OTF, the EFSTEM data shows no depth dependence for a laterally extended object. The microscope was then adjusted to the EFSCEM mode for the same energy loss using the method outlined above, and a z scan repeated for a range of ESW widths, as shown in Fig. 2. The EFSCEM data shows a clear depth dependence.

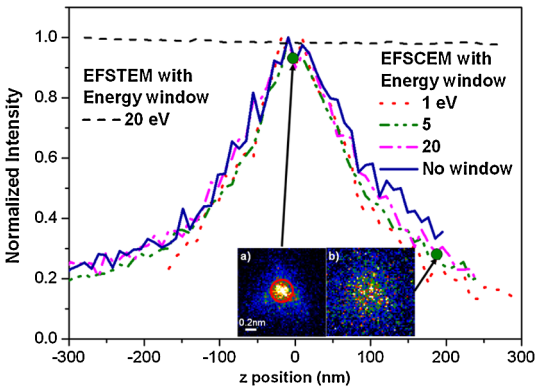

FIG. 2 (color online). 1D EFSCEM optical sectioning of a carbon film along the sample thickness direction using energy selecting windows. EFSTEM optical sectioning is shown for comparison. Inserts show probe images recorded with (a) the sample at the confocal point and (b) 180 nm above it. The red circle in (a) indicates the location of the virtual collector aperture.

Remarkably, Fig. 2 shows that increasing the size of the ESW has minimal effect on the FWHM of the depth dependent signal. The focal spread of the postspecimen optics due to C_c is ~300 nm for a 40 eV ESW but the observed depth resolution even without an ESW is better than this. The EFSCEM experiment is therefore not sensitive to the size of ESW and a corollary to this is that no energy filter is required for EFSCEM experiments.

In a second set of EFSCEM experiments, a purpose designed piezo-driven stage-scanning system [17] was used to acquire 2D lateral (x-y) scans, or alternatively to slice in depth by scanning along one lateral direction and the depth direction to form an (x-z) scan. For these initial experiments, the specimen used was a perforated carbon film decorated with Au nanoparticles and the microscope was adjusted to the confocal mode for the carbon K-edge scattering. Figures 3(a) and 3(d) compare EFSCEM lateral x-y scans acquired with the sample positioned at the confocal height with and without a collector aperture present. In the absence of a collector aperture, all the scattered intensity collected by the postspecimen lens contributes to the image. This configuration is therefore identical to performing conventional EFSTEM and is not confocal. Similarly, Figs. 3(b) and 3(e) compare scans in the x-z plane at positions corresponding to $y = 0$ nm in Figs. 3(a) and 3(d), respectively. No image contrast from the Au nanoparticles was observed as we specifically collected inelastic scattering characteristic of carbon. The depth line profiles along the solid and dashed lines lines L1 and L2 in Figs. 3(b) and 3(e) are shown in Figs. 3(c) and 3(f), respectively.

The FWHMs of the intensity profiles L1 and L2 collected in EFSTEM modes [Fig. 3(c)] are elongated to more than 1 μm. In the EFSCEM mode, rejection of scattering away from the confocal plane occurs and the data shows a

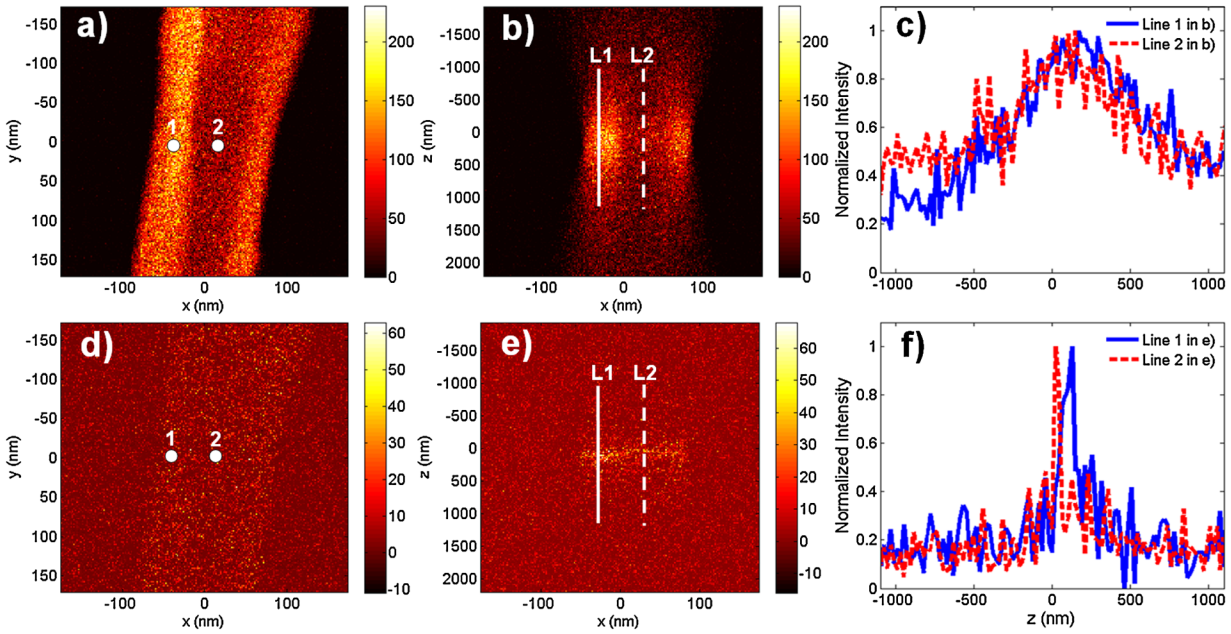

FIG. 3 (color online). EFSCEM x-y scans acquired from a carbon film positioned at the confocal point (a) without a collector aperture and (d) with a collector aperture corresponding to a diameter of 0.32 nm. (b) and (e) EFSCEM x-z scans along $y = 0$ nm in (a) and (d), respectively. (c) and (f) line profiles along the lines L1 and L2 shown in (b) and (e).

FWHM in the depth direction of 84 ± 21 and 42 ± 21 nm at points 1 and 2, respectively, [Fig. 3(f)]. An independent measurement of the thickness of the sample at points 1 and 2 in Fig. 3(a) gave values of 65 ± 7 nm and 32 ± 3 nm, respectively, (see supplementary material [16]). The slightly larger thickness values measured by EFSCEM are expected because the depth resolution under the conditions used is about 15 nm, broadening the image in the depth direction. Direct imaging of the change in thickness and height of the carbon film between points 1 and 2 is demonstrated by this data.

To quantitatively examine the effective depth and energy resolution in EFSCEM, and to explain why the depth resolution is retained in the presence of C_c, we have calculated the plane-spread function or z response, which describes the depth resolution of a laterally extended object. For an infinitely thin and completely incoherent scattering plane, the z response (ignoring C_c) can be written as

$$Z_{\mathrm{SCEM}}(z) = \int |P_1(\mathbf{R}, z)|^2 |P_2(-\mathbf{R}, -z)|^2 d\mathbf{R} \qquad (2)$$

where $P_1(\mathbf{R}, z)$ and $P_2(\mathbf{R}, z)$ are the 3D wave functions (of lateral position vector, $\mathbf{R}$, and depth coordinate z) that describe imaging of an infinitesimal point through either the pre- or postspecimen optics (see, Ref. [13] for a full description). In the presence of C_c, the EFSCEM z response can be written as

$$Z_{\mathrm{SCEM}}(z, \varepsilon) = \int |P_1(\mathbf{R}, z)|^2 \times \left| P_2\left[-\mathbf{R}, -\left(z + \frac{\varepsilon}{E_0} C_{c2}\right)\right]\right|^2 d\mathbf{R} \qquad (3)$$

where a parameter, ε, is included that gives the deviation in the energy of scattered electrons from a specific energy loss ΔE_{loss}. This deviation causes the focal point of the postspecimen optics P_2 to shift away from the focal point of the prespecimen optics P_1 by a distance of $\varepsilon C_{c2}/E_0$.

Figure 4 shows the theoretical EFSCEM z response as a function of sample height, z, and energy deviation, ε, for the experimental conditions described in the supplementary material [16]. Infinitesimal electron source and collector aperture sizes are assumed. To further examine the depth and energy response, the plot shown in Fig. 4 has been projected to form both a z response integrated over all possible electron losses, and an energy-filtering response integrated over all possible heights of a scattering plane. This provides an estimate for the FWHM of the z response at 15.7 nm, and for the energy response at 2.3 eV. Thus only electrons with an energy loss close to ΔE_{loss} for which the confocal trajectory was aligned contribute to the image, which infers that the depth resolution is not significantly degraded by C_c. Because of the C_c of the postspecimen lens, electrons at other energy losses will be focused at the image plane collector aperture only if they arise from scattering above or below the nominal confocal point. However, such points are not strongly illuminated by the focused beam formed by the prespecimen optics, and the signal from these points is therefore suppressed. We therefore conclude that the C_c of the postsample lens provides energy selectivity in addition to the observed depth selectivity.

In conclusion, we have described a method for establishing optical trajectories required for EFSCEM. We have also presented the first data measuring the z response in

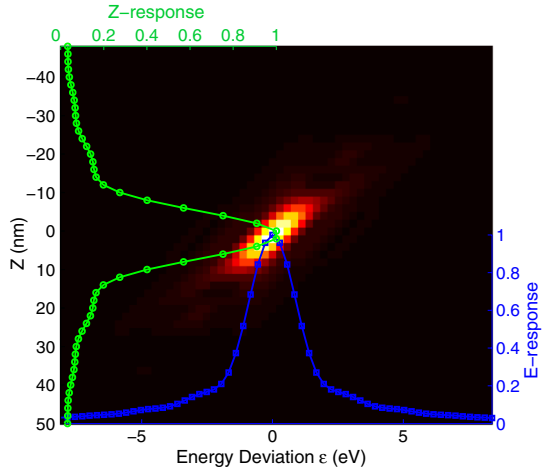

FIG. 4 (color online). 2D plot of the EFSCEM z response as a function of sample height, z, and energy deviation ε of electrons scattered by the sample. Overlaid curves (-○-) and (-□-) show projections formed by projecting the z response along the energy deviation and z directions, respectively.

this mode and have demonstrated that it is not limited by C_c. Moreover, we have shown that residual C_c provides an energy selection effect in EFSCEM and determines the energy resolution. Therefore an energy filter or C_c corrector is not necessary for this imaging mode, greatly expanding its applicability. We have performed EFSCEM optical sectioning experiments using a laterally extended object sample, which shows that the depth resolution is greatly improved over the conventional STEM geometry.

Although the depth resolution demonstrated here is not yet comparable to that obtained using electron tomography [18], the current data acquisition process is much faster and minimal data processing is required to retrieve the 3D information. In general, electron tomography also suffers from a missing wedge in the transfer function, unlike the confocal approach, which reduces the z response for laterally extended objects unless a specially prepared needle sample that allows a full 180° rotation is used. Although x-ray tomography has been used to reconstruct relatively large 3D structures [19], the wavelength of x-rays, and the relatively poor quality of x-ray lenses, leads to a limiting resolution of 30 nm in practice. The position sensitive atom probe [20] allows single atom counting of a 3D structure. However, samples need to be fabricated into sharp needles, and because this technique counts individual atoms, the analyzed volume is limited to about 10^6 nm^3 (100 nm in diameter by 100 nm in depth) with a data collection time of several hours [21].

Our methodology assumes that only defocus varies as a function of energy loss, and that other aberrations are unchanged. In practice this may be an approximation that leads to a reduction in the achievable depth and energy resolution. We further note that the experimental depth resolutions achieved in this work differ between for the 1D and 2D scans. The 1D scans reported here were recorded using an older and slower piezo drive, and drift in the aberrations or sample may have affected the measurements.

The authors would like to thank Dr. Andrew Bleloch for open and helpful discussions. G. B. would like to thank Intel Ireland Ltd for financial support. P. W., A. I. K., and P. D. N. acknowledge financial support from the Leverhulme Trust (F/08 749/B) and the EPSRC (EP/F048009/1). Technical assistance from JEOL Ltd and JEOL (UK) Ltd is also acknowledged. Part of this work was supported by the Japan Society for the Promotion of Science, Japan-UK Research Cooperative Program. K. M. and A. H. acknowledge financial support from a Grant-in-Aid for Scientific Research (C) 2009-218577 and for Young Scientists (B) 20760027, respectively.

*Corresponding author.
peter.nellist@materials.ox.ac.uk

[1] M. Gu, *Principles of Three Dimensional Imaging in Confocal Microscopes* (World Scientific, Singapore, 1996).
[2] S. P. Frigo, Z. H. Levine, and N. J. Zaluzec, Appl. Phys. Lett. **81**, 2112 (2002).
[3] O. Scherzer, Z. Phys. **101**, 593 (1936).
[4] M. Haider *et al.*, J. Electron Microsc. **47**, 395 (1998).
[5] O. L. Krivanek, N. Dellby, and A. R. Lupini, Ultramicroscopy **78**, 1 (1999).
[6] P. D. Nellist *et al.*, Science **305**, 1741 (2004).
[7] K. van Benthem *et al.*, Appl. Phys. Lett. **87**, 034104 (2005).
[8] G. Behan *et al.*, Phil. Trans. R. Soc. A (to be published).
[9] B. R. Frieden, J. Opt. Soc. Am. A **57**, 56 (1967).
[10] H. L. Xin and D. A. Muller, J. Electron Microsc. **58**, 157 (2009).
[11] P. D. Nellist *et al.*, Appl. Phys. Lett. **89**, 124105 (2006).
[12] E. C. Cosgriff *et al.*, Ultramicroscopy **108**, 1558 (2008).
[13] A. J. D'Alfonso *et al.*, Ultramicroscopy **108**, 1567 (2008).
[14] M. Haider *et al.*, Ultramicroscopy **108**, 167 (2008).
[15] H. Rose, Ultramicroscopy **103**, 1 (2005).
[16] See supplementary information at http://link.aps.org/supplemental/10.1103/PhysRevLett.104.200801.
[17] M. Takeguchi *et al.*, J. Electron Microsc. **57**, 123 (2008).
[18] P. A. Midgley and M. Weyland, Ultramicroscopy **96**, 413 (2003).
[19] B. P. Flannery *et al.*, Science **237**, 1439 (1987).
[20] M. K. Miller, *Atom-probetomography* (Kluwer Academic/Plenum Publishers, New York, 2000).
[21] F. K. Thomas and K. M. Michael, Rev. Sci. Instrum. **78**, 031101 (2007).